
Final Report

Project Title: 10 MW Supercritical CO₂ Turbine Test

Project Period: 10/01/12 – 10/31/13

Project Budget: \$1,799,974

Submission Date: 01/27/2014

Recipient: National Renewable Energy Laboratory

Address: 15013 Denver West Parkway
Golden, CO 80401

Award Number: DE-EE0001589

Awarding Agency: DOE EERE SETP CSP subprogram

Project Team: Sandia National Laboratories
University of Wisconsin at Madison
Echogen Power Systems
Barber-Nichols, Inc.
Abengoa Solar
Electric Power Research Institute

Cost-Sharing Partners: Echogen Power Systems
Abengoa Solar
Electric Power Research Institute

Principal Investigator: Craig Turchi, PhD
Senior Engineer
Phone: 303-384-7565
Fax: 303-384-7495
Email: craig.turchi@nrel.gov

GO Contracting Officer: Golden, CO

Tech. Project Officer: Christine Bing

DOE Technical Mgr.: Mark Lausten

Executive Summary

The goal of this project was to demonstrate the inherent efficiencies of a supercritical carbon dioxide (s-CO₂) power turbine and associated turbomachinery under conditions and at a scale relevant to commercial concentrating solar power (CSP) projects, thereby accelerating the commercial deployment of this new power generation technology. The project involved eight partnering organizations: NREL, Sandia National Laboratories, Echogen Power Systems, Abengoa Solar, University of Wisconsin at Madison (UW-Madison), Electric Power Research Institute (EPRI), Barber-Nichols, and the CSP Program of the U.S. Department of Energy (DOE).

The multi-year project planned to design, fabricate, and validate an s-CO₂ power turbine of nominally 10 MWe that is capable of operation at up to 700°C and operates in a dry-cooled test loop. Many stakeholders are interested in the potential of the s-CO₂ Brayton cycle; for solar applications, advanced s-CO₂ Brayton cycles have the potential to achieve the SunShot goal of greater than 50% thermal-to-electric conversion efficiency.

The project plan consisted of three phases. System design and modeling occurred in Phase 1, followed by fabrication in Phase 2, and testing in Phase 3. The major accomplishments of Phase 1 included:

- Design of a multistage, axial-flow s-CO₂ power turbine,
- Design modifications to an existing turbocompressor to provide s-CO₂ flow for the test system,
- Updated equipment and installation costs for the turbomachinery and associated support infrastructure,
- Development of simulation tools for the test loop itself and for more efficient cycle designs that are of greater commercial interest,
- Simulation of s-CO₂ power cycle integration into molten nitrate salt CSP systems indicating a cost benefit of up to 8% in LCOE,
- Identification of recuperator cost as a key economic parameter,
- Corrosion data for multiple alloys at temperatures up to 650°C in high-pressure CO₂ and recommendations for materials-of-construction, and
- Revised test plan and preliminary operating conditions based on the ongoing tests of related equipment.

This report describes the progress made during Phase 1 and compares Phase 1 results to the stated milestones. The report then outlines proposed modifications to the original statement of project objectives (SOPO) designed to achieve the primary goal and major objectives of the project while staying within the funding provided by the four contributing organizations.

Phase 1 established that the cost of the facility needed to test the power turbine at its full power and temperature would exceed the planned funding for Phases 2 and 3. The team proposed to derate the test facility from 700°C to 600°C to save on materials cost and presented this alternative to DOE. Toward the end of Phase 1 a unique opportunity

arose to collaborate with another turbine development team to construct a single, shared s-CO₂ test facility. The synergy of the combined effort would result in greater facility capabilities than either separate project could produce and would allow for testing of both turbine designs within the combined budgets of the two projects. All industry partners in both projects supported the collaborative effort. Subsequently, the project team requested a no-cost extension to Phase 1 to develop a Phase 2 proposal based on this collaborative approach. DOE allowed a brief extension for reasons unrelated to the proposed collaboration, but ultimately opted not to pursue the collaborative facility and terminated the project.

Table of Contents

| | |
|---|----|
| Executive Summary | 2 |
| Background | 4 |
| Introduction | 5 |
| Phase 1 Milestones | 6 |
| Project Results and Discussion | 9 |
| Task 1.1 Corrosion and Materials Analysis..... | 9 |
| Alloy IN800H | 10 |
| 347SS | 11 |
| AFA-OC6 | 12 |
| Haynes 230..... | 14 |
| 316SS & 310SS | 14 |
| Ferritic-martensitic Steels | 15 |
| Summary of Phase 1 Materials Tests | 15 |
| Task 1.2 Test Plan Development..... | 16 |
| Task 1.3 Test Loop Design..... | 18 |
| Power Turbine Design | 19 |
| Materials | 20 |
| High Temperature Recuperator | 21 |
| Heat Rejection System..... | 21 |
| Heat Addition System..... | 22 |
| Task 1.4 Modeling and Simulation of Cycles | 23 |
| Task 1.5 Commercial Power Cycle..... | 23 |
| Task 1.6 CSP Commercial Deployment Path | 25 |
| S-CO ₂ Cycle Design-Point Modeling | 25 |
| Off-Design S-CO ₂ Cycle Modeling..... | 25 |
| CSP S-CO ₂ Annual Simulations | 26 |
| CSP Roadmap | 27 |
| Utility Stakeholder Workshop | 28 |
| Task 1.7 Site Preparation | 28 |
| Conclusions..... | 30 |
| Path Forward:..... | 31 |
| References:..... | 33 |

Background

Power cycle efficiency has a dramatic impact on CSP levelized cost. Higher efficiency in the power cycle reduces the size and cost of the solar field and thermal storage system required to achieve the desired system capacity and reduces the size of the power block cooling loads. Higher efficiency in the power cycle also reduces plant size and associated environmental footprint.

The current state of the art in CSP technology is the molten salt power tower. Although power towers are capable of achieving temperatures up to 900°C, the molten nitrate salt used as the heat transfer and thermal storage fluid is limited to temperatures less than about 600°C. An operating limit of approximately 565°C, combined with a dry-cooled steam Rankine power cycle, limits thermal-to-electric conversion efficiency to approximately 41%.

This project planned to showcase the turbomachinery for a new cycle, the s-CO₂ Brayton cycle, capable of achieving DOE SunShot objectives of greater than 50% dry-cooled efficiency with a power block cost less than \$1200/kW. Originally proposed in the late 1960s [1], this cycle has been under renewed investigation for the past decade [2-6]. Researchers have modeled the basic thermodynamics of the cycle and used small test rigs to explore the behavior of s-CO₂ turbomachinery and operational characteristics of a closed Brayton cycle [7]. However, validation via operation of a larger-scale prototype at temperatures relevant to CSP is needed to establish the true potential of the power cycle.

While s-CO₂ power cycles hold much promise for CSP systems, there are numerous hurdles to overcome before commercial s-CO₂ Brayton cycles achieve the efficiency and reliability necessary for the solar application. No systems have been designed and tested at turbine inlet temperatures greater than about 500°C. Better understanding of material selection and corrosion mechanisms at higher temperatures, thermal stress management, and real-gas aerodynamic performance modeling are all critical design issues that will benefit from the execution of this program. Similarly, compressor designs matched to dry cooling conditions are required.

Fortunately, we are able to draw on a substantial body of existing work. Over the past several years, research teams from around the world have proposed and modeled thermodynamic cycles using s-CO₂. Laboratory and small-scale test systems have been assembled to explore the behavior of s-CO₂ when compressed near and through the critical point, and the operation of small-scale s-CO₂ turbomachinery and heat exchangers in a closed loop cycle. Members of this proposal team have been heavily involved in this preliminary development work, as indicated by their organization and participation in two symposia devoted specifically to the s-CO₂ power cycles in 2009 and 2011.

Figure 1 shows how applicability of major system components varies with overall scale. Considering bearings, seals, rotational speed, and ancillary equipment, a nominal 10-MWe capacity is estimated to be the minimum size that allows for a viable commercial design of the power turbine [8]. The commercial potential of the s-CO₂ turbine cannot be evaluated unless high-efficiency, commercial-scale design elements can be

incorporated in the unit and this project will validate the performance of a commercial-scale, high-temperature s-CO₂ turbine.

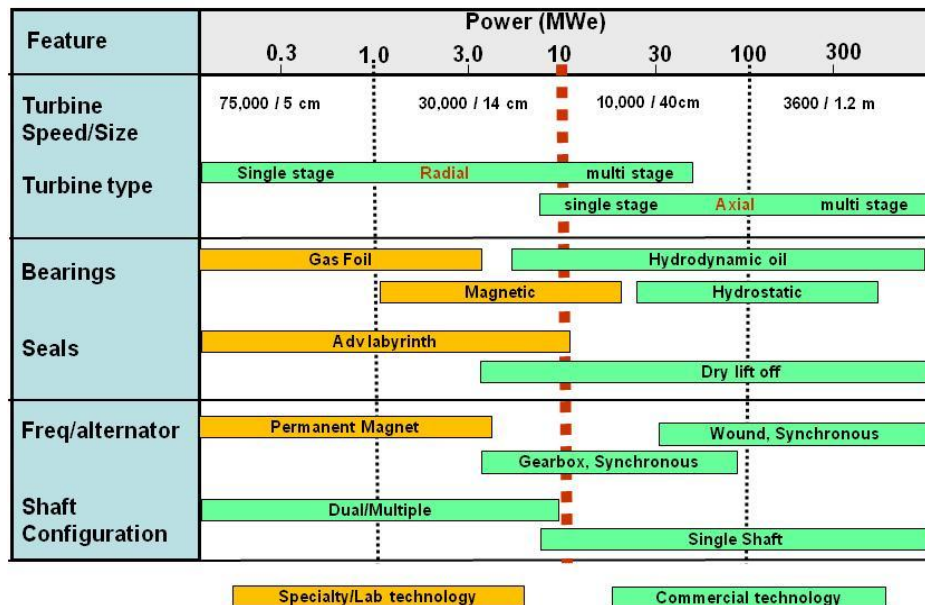


Figure 1. Range of applicability of turbomachinery features. Use of commercial design elements is essential for efficiency and reliability while reducing cost. Adapted from [8].

Introduction

Commercial demonstration of the s-CO₂ Brayton cycle is imminent, although not for the conditions necessary for CSP. Project member Echogen fielded a 250-kW prototype system in 2010 and started testing of the larger EPS100 in 2012. The EPS100 is designed to run at temperatures of approximately 500°C and with wet cooling, and the knowledge and support infrastructure developed for the EPS100 was leveraged for this project. The ability to tap into Echogen’s existing knowledge base for instruments and controls, ancillary equipment, and skid layout significantly reduced the cost for design and testing of an s-CO₂ turbine of the necessary scale.

The goal of the three-phase project was to demonstrate the efficiency of s-CO₂ turbomachinery and operation of the power cycle under conditions relevant to CSP – including high turbine inlet temperatures, high compressor inlet temperatures (indicative of dry cooling), and frequent transient operation. Testing the turbomachinery requires assembling a full power cycle with the associated ancillary facilities for heat supply and rejection, CO₂ supply, controls, and safety. The overall project tasks and team roles are outlined in Table 1.

The project requires the team to specify and construct the power turbine and requisite compressors and ancillary equipment necessary for a complete power conversion system. The prototype would validate turbomachinery efficiency and cycle response to transient operation and dry cooling conditions. Concurrently, the team would refine performance models that predict steady-state and transient system response. Experimental data would be used to validate the models, and simulations would be made of one or more advanced cycle configurations that achieve a power block

efficiency of greater than 50% and power block cost less than \$1,200/kW, in accordance with the SunShot targets. The project would dramatically advance the understanding of this disruptive technology by building upon prior laboratory-scale work and developing, deploying and testing a prototype system. Altogether, the project team was uniquely qualified not only to develop and test the s-CO₂ power cycle, but to take the technology forward into the marketplace.

Table 1. Project tasks and partner roles.

| Task | Phase 1 – Design (10/1/12 – 9/30/13) | Task Lead |
|------|---|-------------|
| 1-1 | Corrosion and materials analysis | UW-Madison |
| 1-2 | Test plan development | NREL |
| 1-3 | Test loop design | Echogen |
| 1-4 | Modeling and simulation of cycles | NREL |
| 1-5 | Commercial power cycle | Echogen/D-R |
| 1-6 | CSP commercial deployment path | Abengoa |
| 1-7 | Site preparation | Sandia |
| | Phase 2 – Fabrication & Installation (10/1/13 – 1/15/15) | |
| 2-1 | Corrosion and materials analysis (cont.) | UW-Madison |
| 2-2 | Test loop construction | Echogen/D-R |
| 2-3 | Installation and check-out | Sandia |
| 2-4 | Modeling and simulation | NREL |
| 2-5 | Conceptual design study of Commercial CSP system | Abengoa |
| | Phase 3 – Testing & Simulation (1/15/15 – 12/30/15) | |
| 3-1 | Corrosion and materials analysis (cont.) | UW-Madison |
| 3-2 | Low-temp operation | Sandia |
| 3-3 | High-temp operation | Sandia |
| 3-4 | System model validation | NREL |
| 3-5 | Response and control of recompression cycle | Sandia |

Phase 1 Milestones

The Phase 1 milestones are taken directly from the statement of project objectives (SOPO) below. The progress toward and accomplishment of these milestones is discussed in the following sections.

- Milestone (Task 1.1):** Produce a matrix of candidate materials showing their corrosion performance at time intervals of 1000 hours over the range of operating conditions from 300°C to 650°C, up to 200 bar. Identify qualifying materials which meet corrosion (<30 microns/yr) validated with TEM or SEM at the anticipated operating temperature of the test unit. From this set of identified materials, recommend materials of construction for the test system based upon ranked factors including cost. Submit for publication the interim findings and the theory for predicted corrosion behavior up to 750°C based on the correlated data and fundamental material mechanisms.

- **Milestone (Task 1.2):** Test Plan and draft SOP. SOP will be reviewed and finalized during Phase 2. The SOP will include calibration protocols and data review procedures to ensure overall data quality.
- **Milestone (Task 1.3.1):** Manufacturing design specifications for a turbo-expander with an 80% isentropic design-point efficiency and a compressor with an 80% isentropic design-point efficiency and all components listed above including a manufacturer's turbomachinery design of the following design performance parameters:
 - a. flow path geometry,
 - b. turbine shaft speed and resultant gear ratio to synchronous power generation speed,
 - c. steady-state turbine thrust load as a percentage of bearing capability,
 - d. turbine shaft seal leakage rates, absolute and relative to total working fluid load and flow rate,
 - e. turbine bearing heat generation rates, absolute and relative to total developed shaft power,
 - f. overall power conversion efficiency (isentropic power to turbine shaft power, turbine shaft power to generator shaft power, generator shaft power to generator electrical power at the generator terminals).
- **Milestone (Task 1.3.2):** A manufacturer's turbo-machinery design study in which projects the following design performance parameters of a 100 MW s-CO₂ power block:
 - a. turbine shaft seal leakage rates, absolute and relative to total working fluid load and flow rate,
 - b. turbine bearing heat generation rates, absolute and relative to total developed shaft power, and
 - c. overall power conversion efficiency (isentropic power to turbine shaft power, turbine shaft power to generator shaft power, generator shaft power to generator electrical power at the generator terminals).
- **Milestone (Subtask 1.4.1):** Transient performance model for the 10 MW test loop capable of tracking 1-minute deviations in system conditions.
- **Milestone (Task 1.5):** Present the proposed commercial cycle design applicable to CSP for first deployment with a dry-cooled power block with costs which demonstrates market viability and are less than \$1200/kW with thermal-to-electric efficiency greater than 44%. Report to DOE on commercial power cycle design efforts to address CSP integration requirements.
- **Milestone (Task 1.6):** Report on evaluated s-CO₂ integrated CSP systems comparing estimated cost and performance characteristics including annual and peak efficiency, installation cost, LCOE, solar and thermal efficiency, capacity factor, generation profile and scale.
- **Milestone (Task 1.7):** Complete assessment of NEPA and permit modifications necessary for installation of the 10 MW test system at the Sandia site. Develop timeline and work assignments necessary for completing these requirements by the target Phase 2 installation date.

Go/No-Go Decision Phase 1

Successful completion of all Phase 1 milestones, including:

- An s-CO₂ cycle design which modeling shows achieves 50% thermal-to-electric efficiency.
- A turbine design with the details on the materials, geometry and operating parameters for the test loop which modeling shows achieves 80% isentropic efficiency.
- A proposed commercial power cycle design with a design study which projects performance from this 10 MW Turbine project to a 100 MW sCO₂ power block (documented under Task 1.5), an assessment of the design features and level of effort to implement those features for commercial CSP power cycle deployment, and demonstration of the cost-performance-risk market viability of the power cycle for CSP (Task 1.5),
- An identified CSP s-CO₂ plant configuration which meets SunShot targets and a demonstration and deployment plan to achieve commercial success (Task 1.6).
- A transient performance model for the 10MW test loop (Task 1.4).

As a result of the go/no-go or stage-gate or continuation reviews, DOE may, at its sole discretion, make any of the following determinations: (1) continue to fund the project, depending on the availability of appropriations; (2) recommend specific direction or redirection of work under the project; (3) place a hold on the project pending further supporting data, funding, or to evaluate other projects concurrently; or (4) stop funding the project due to noncompliance, insufficient progress, inadequate business plan, schedule slip, change in strategic direction, or other factors.

Project Results and Discussion

Task 1.1 Corrosion and Materials Analysis

Under Task 1.1 team member UW-Madison tested several commercial alloys for their suitability in s-CO₂ at various conditions. The alloys selected for testing and the Phase 1 test conditions are shown in Table 2. Ongoing discussion during Phase 1 and available space in the test chamber led to the inclusion of a couple additional test cases during Phase 1, as shown in Table 2. Compositions of the alloys are provided in Table 3.

Table 2. Matrix of Test Conditions & Materials.

| Test | Temp. | Press. | Gas | Mat1 | Mat2 | Mat3 | Mat4 | Mat5 |
|--|--------|--------|---|-------|-------|------------|--------|---------|
| 1 | 450°C | 20 MPa | Research grade CO ₂ (99.9998%) | 316SS | 347SS | Haynes 230 | IN800H | AFA-OC6 |
| 2 | 550°C | 20 MPa | | 316SS | 347SS | Haynes 230 | IN800H | AFA-OC6 |
| 3 | 650°C | 20 MPa | | IN740 | 347SS | Haynes 230 | IN800H | AFA-OC6 |
| Additional alloys added to the test regime during Phase 1: | | | | | | | | |
| 4 | 650°C | 20 MPa | Research grade CO ₂ (99.9998%) | 316SS | 310SS | Haynes 282 | IN617 | |
| 5 | <600°C | 20 MPa | | P91 | NF616 | HCMA12A | | |

Table 3. Elemental Composition (wt. %) of Candidate Alloys

| | NF616 | HCM A12A | P91 | AFA-OC6 | 316 SS | 347 SS | 310 SS | IN 800H | IN 617 | Haynes 230 | IN740 | Haynes 282 |
|-------|-------|----------|-------|---------|--------|--------|--------|---------|--------|------------|--------|------------|
| Fe | Bal. | Bal. | 89.1 | Bal. | Bal. | Bal. | Bal. | Bal. | <2 | 3.0** | 0.1491 | 0.79 |
| Cr | 8.82 | 10.83 | 8.4 | 13.84 | 17.4 | 17.67 | 25 | 19.63 | 22 | 22.0 | 24.57 | 19.40 |
| Ni | 0.17 | 0.39 | .21 | 25.04 | 13.3 | 9.62 | 21.5 | 33.17 | 52 | Bal. | 50.04 | Bal. |
| Al | 0.005 | 0.001 | 0.022 | 3.56 | - | - | - | 0.46 | 1.2 | 0.3 | 1.33 | 1.58 |
| Mn | 0.45 | 0.64 | 0.45 | 1.99 | 1.7 | 1.66 | 2 | 0.77 | 0.5 | 0.5 | 0.245 | 0.04 |
| Nb | 0.06 | 0.05 | 0.076 | 2.51 | - | 0.72 | - | - | 0.08 | - | 1.46 | <0.1 |
| Cu | - | 1.02 | 0.17 | 0.51 | - | 0.38 | - | 0.20 | 0.5 | - | 0.015 | <0.01 |
| Mo | 0.46 | 0.30 | 0.9 | 0.18 | 2.7 | 0.38 | - | - | 9 | 2.0 | 0.35 | 8.52 |
| Si | 0.10 | 0.27 | 0.28 | 0.13 | 0.43 | 0.77 | 1 | 0.29 | 1.2 | 0.4 | 0.17 | <0.05 |
| C | 0.11 | 0.11 | 0.10 | 0.114 | 0.045 | 0.051 | 0.25 | 0.06 | - | 0.10 | 0.023 | 0.061 |
| W | 1.87 | 1.89 | - | 0.16 | - | - | - | - | - | 14.0 | 0.022 | <0.01 |
| Ti | - | - | - | 0.05 | - | - | - | 0.53 | 0.3 | - | 1.33 | 2.08 |
| V | 0.19 | 0.19 | 0.22 | 0.05 | - | - | - | - | - | - | 0.012 | - |
| P | - | - | - | 0.022 | - | 0.027 | 0.04 | - | - | - | 0.0023 | <0.002 |
| N | - | 0.06 | 0.048 | 0.001 | 0.044 | - | - | - | - | - | 0.0038 | - |
| B | - | - | - | 0.008 | - | - | - | - | 0.006 | - | 0.0013 | 0.004 |
| Zr | - | - | - | - | - | - | - | - | - | - | 0.021 | <0.002 |
| Co | - | - | - | - | - | 0.20 | - | - | 12.5 | 5.0** | 20.09 | 10.37 |
| Ta | - | - | - | - | - | 0.021 | - | - | - | - | 0.004 | <0.01 |
| La | - | - | - | - | - | - | - | - | - | - | - | - |
| S | - | - | - | 0.001 | - | 0.024 | 0.03 | <0.001 | - | - | 0.003 | <0.002 |
| Other | | | | - | B, S | - | - | - | - | B, La | - | - |

The summary of results of the weight gain measurements and some surface and cross sectional analysis is presented below. Oxidation curves fitted to the measured data points describing the reaction kinetics are also shown along with error bars at each measured data point. Uncertainty values are computed using ASTM Manual 7 on Presentation of Data and Control Chart Analysis (6th Ed.), Table 2, pg. 39, which uses a student t table recomputed from R.A. Fisher's book, and for this study is computed

based on 95% confidence limits. Results have been submitted to *Corrosion Science* [16, 17].

Alloy IN800H

The weight gain values and surface morphology of the austenitic alloy 800H are shown below in Figure 2 and SEM micrographs in Figure 3. Alloy 800H performed better than 347SS at 650°C, but no better than 347SS at 550°C. 800H alloy has high chromium (20% Cr) and nickel (33% Ni) content, which contributes to its strong performance. It is noteworthy to mention that alloy 800H exhibited a continuous parabolic trend with increasing temperature, which was found to consist of a thin protective oxide layer up to 650°C. Nodular islands of oxide phases did begin to form at 450°C and continue to grow very slowly with exposure time and temperature. 800H displayed very few oxide islands, most of which nucleated from titanium precipitates on the surface. Resistance to corrosion was very good.

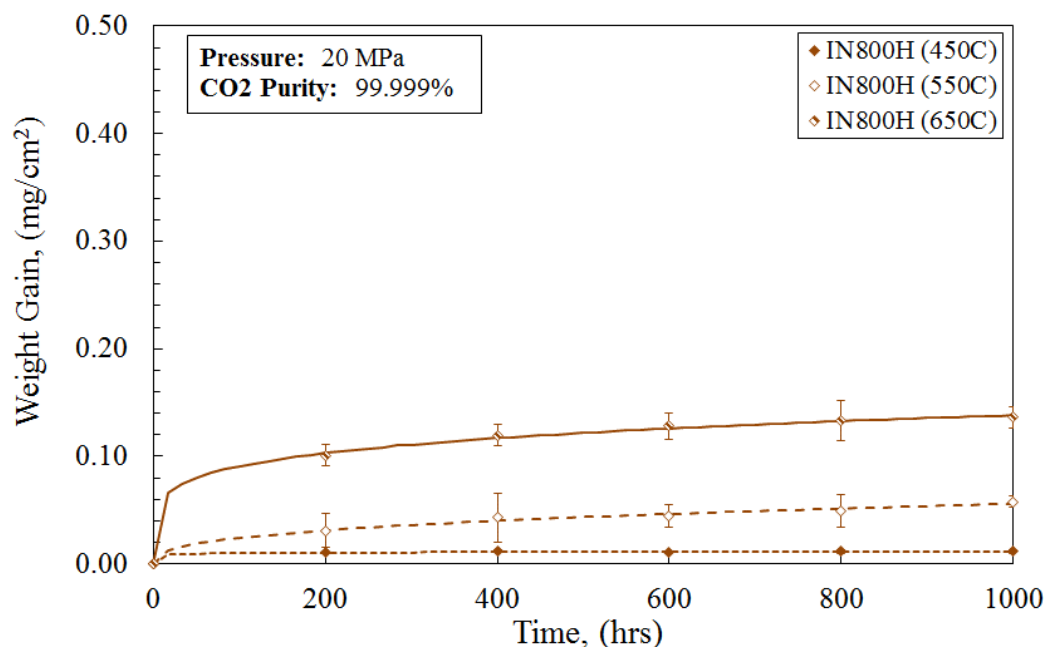


Figure 2. Oxidation curves of alloy 800H at 450°C, 550°C, and 650°C in research grade s-CO₂.

At elevated temperatures, alloy 800H offers resistance to oxidation, carburization, and sulfidation along with rupture and creep strength. In general, nickel based alloys are more resistant to carburization than lower nickel alloys. An Arrhenius plot of the oxidation rate constant for alloy 800H yielded a straight line relationship.

Energy Dispersive Spectroscopy (EDS) maps for alloy 800H reveal a chromium oxide outer layer with an inner layer depleted in chromium. The chromium oxide average thickness was found to be about 1-3 μm . Areas of increased oxidation occurred around titanium rich zones allowing oxygen to penetrate beneath the metal surface and enabling an outer iron-oxide growth.

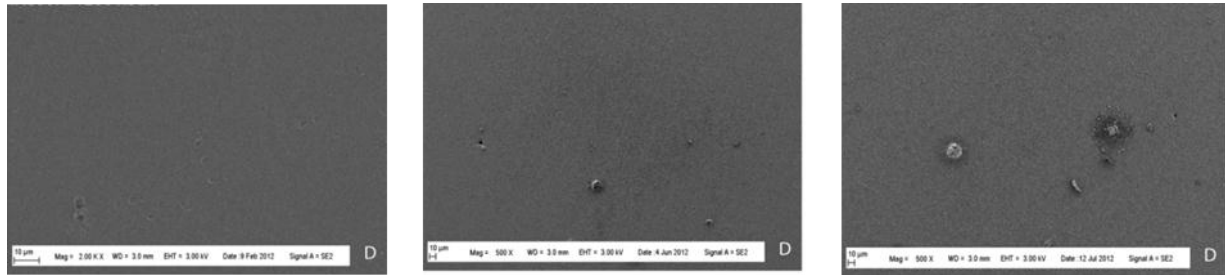


Figure 3. Surface morphology of alloy 800H at 2000X after 1000 hours exposure, from left to right at 450°C, 550°C, and 650°C

347SS

The weight gain and surface morphology of the austenitic alloy 347SS are shown below in Figure 4 and SEM micrographs in Figure 5.

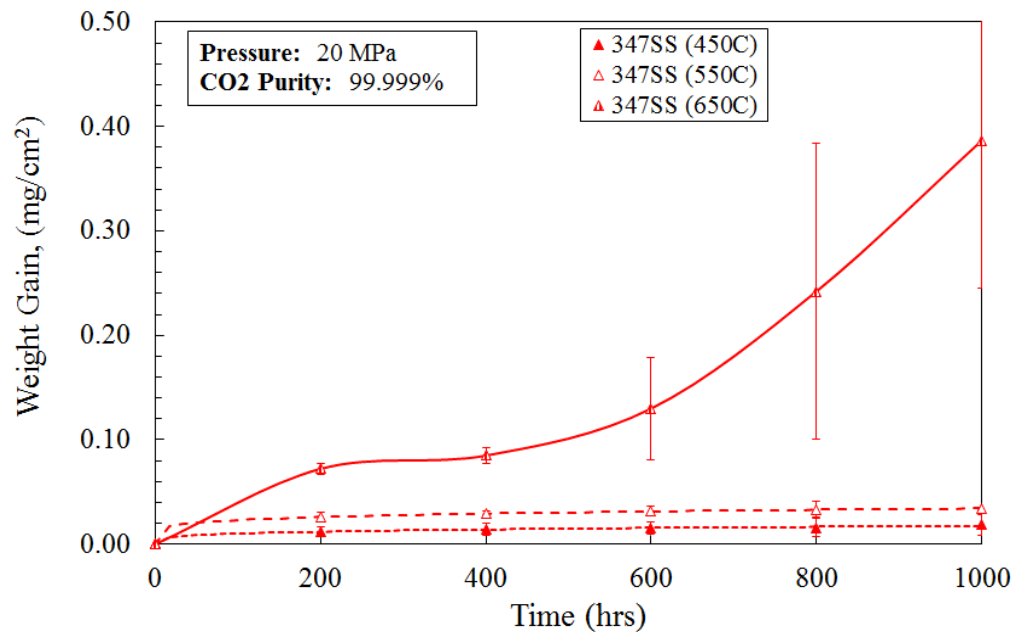


Figure 4. Oxidation curves of 347SS at 450C, 550C, and 650C in research grade s-CO₂.

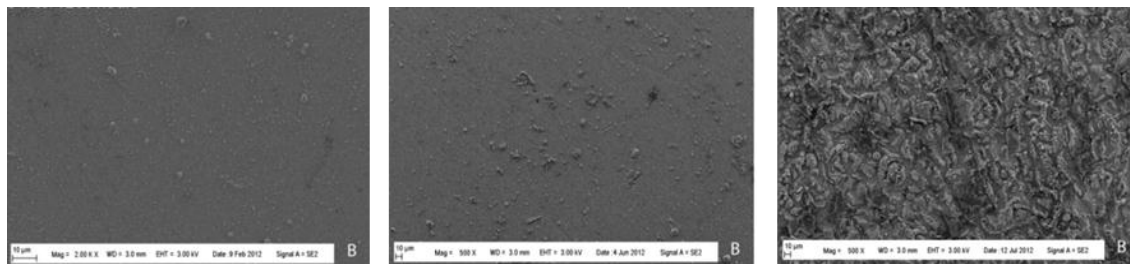


Figure 5. Surface morphology of alloy 347SS at 2000X after 1000 hours exposure, from left to right at: 450°C, 550°C, and 650°C.

347SS exhibited very good protective oxidation similar to alloy 800H through 550°C. Oxide layers were found to be very thin, uniform, fine grained, and fully adherent. EDS analysis indicated nodules of larger oxide growth (oxide islands) that tended to show

signs of increased carbon, as well as being high in niobium. This was expected as niobium is added to prevent sensitization, and will readily form carbides before chromium. This presence of Nb in 347SS was found to have a significant benefit compared to corrosion of 316SS. However, at 650°C the reaction kinetics exhibit breakaway, non-protective oxidation beginning at roughly 400 hours. SEM micrographs providing evidence of this phenomenon can be seen below in Figure 6.

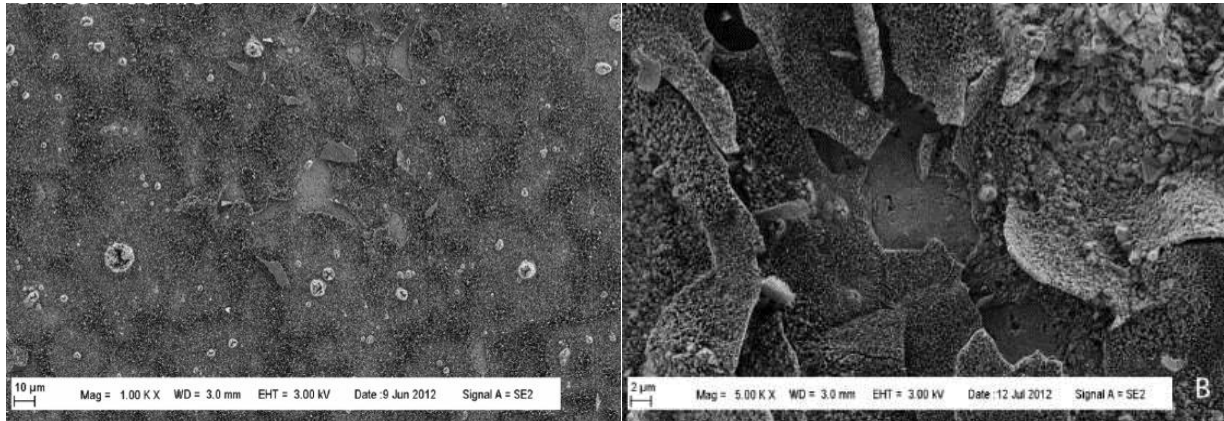


Figure 6. Surface morphology of 347SS at 650°C showing areas of chromia breaking free from the sample surface after (left) 400 hours and (right) 1000 hours exposure. Right-hand image is increased magnification.

EDS analysis showed areas of oxides of chromium (chromia) breaking free from the sample surface at 400 hours, coinciding with the inflection point on the weight gain curve where breakaway oxidation begins. Transitions in the oxidation curve (weight gain) have been explained and described for the stages of oxidation and their characteristic features for CO₂ and CO₂+C environments in previous work [10-11]. Further analysis on an overturned spalled oxide layer fragment showed increased carbon and manganese on the backside. EDS cross-sectional analysis of 347SS found an outer chromia layer, and a corresponding inner layer that was depleted of chromium (iron enriched). The chromium oxide thickness was found to exist in the range of 3-5 μm. Chromium therefore diffused outward to form the protective chromia layer, leaving the adjacent bulk metal matrix depleted. Failure of the oxide layer occurred in part because chromium was no longer available for protective oxide formation. Where the chromia layer failed, oxidation of iron was allowed to occur.

AFA-OC6

The weight gain and surface morphology of the advanced forming austenitic alloy AFA-OC6 at 450°C, 550°C, and 650°C are shown below Figure 7 and in SEM micrographs (Figure 8). Unlike 800H, 347SS and AFA-OC6 did not obey the Arrhenius law. Their weight-gain curves were described by different rate equations with temperature, especially at 650°C where abrupt changes in the oxidation trend occurred for AFA-OC6, which may signify changes in the oxidation mechanism. The fact that the alloys did not obey the Arrhenius law is consistent with Was and Teyseyre who mentioned that in supercritical water virtually no free radical reaction rates follow an Arrhenius law [9].

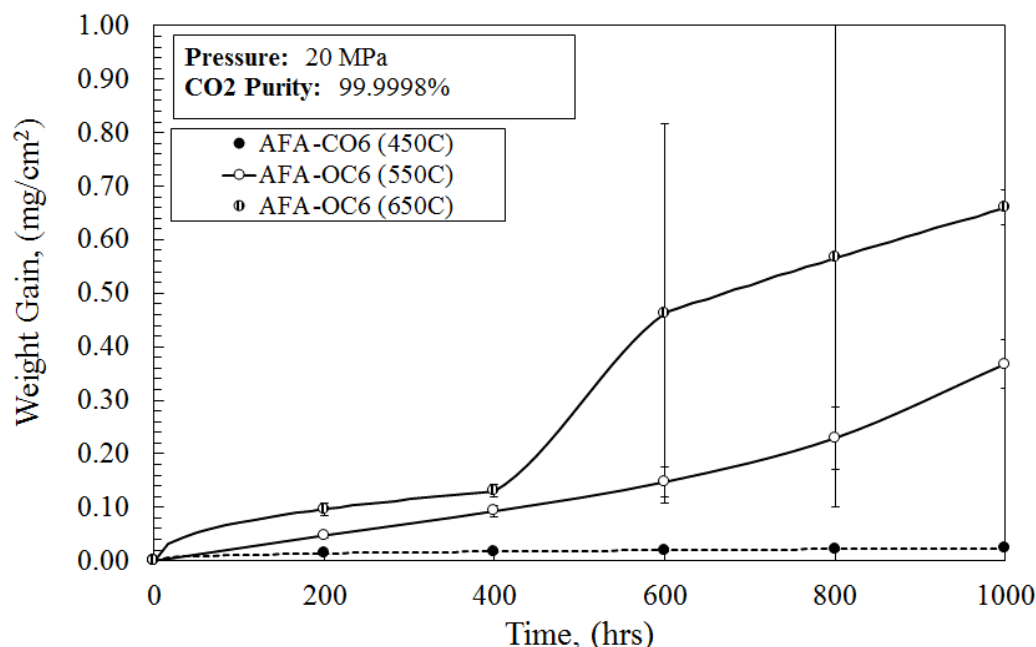


Figure 7. Oxidation curves of AFA-OC6 at 450C, 550C, and 650C in research grade s-CO₂.

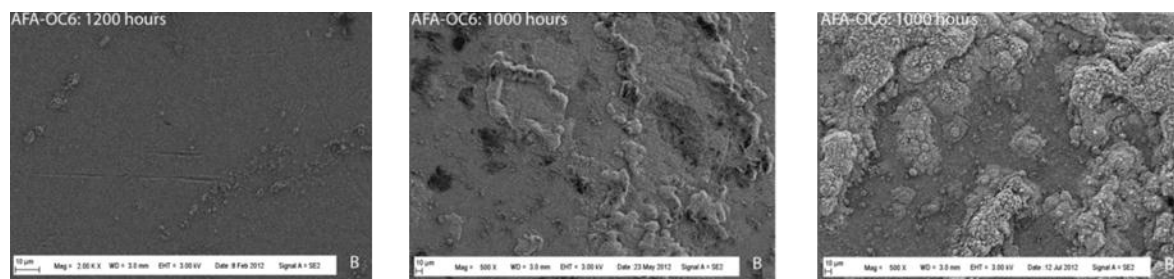


Figure 8. Surface morphology of AFA-OC6 at 2000X after 1000 hours exposure, from left to right at: 450°C, 550°C, and 650°C.

AFA-OC6 exhibited good, protective oxidation at 450°C. The oxide layer was found to be very thin. However, AFA-OC6 exhibited more rapid weight gain and oxide growth than alloy 800H and 347SS at and above 550°C, which can be seen by comparing the previous figures. At 550°C, SEM and EDS analysis revealed dark areas on the surface that correlated to an increase in carbon or carbon deposit, as well as some non-dark areas that showed higher levels of niobium. AFA-OC6 was the only alloy that manifested areas of increased carbon (carbon deposits) and small pit-like areas of material loss. Such features are consistent with the metal dusting mechanism. Metal dusting and carbon deposits on similar alumina-forming austenitic materials have also been reported at 650°C, but in a 50% CO / 49% H₂ / 1% H₂O environment [12].

The weight gain curve for AFA-OC6 exhibits a more S-shaped curve at 650°C. This type of curve is a combination of rate equations employed to describe the behavior or stages of oxidation. Whereas 347SS displayed both breakaway and post-breakaway oxidation at 650°C, AFA-OC6 experienced a ballooning effect in weight gain that remained non-protective. SEM micrographs of AFA-OC6 show large oxide growth. Cross-sectional analysis also indicates non-protective growth to be generally duplex with an iron oxide

outer layer. EDS spectral maps show heavily oxidized areas as mostly iron oxide with some indication of increased carbon.

Haynes 230

Figure 9 shows SEM plan and cross-sectional image views of the oxide layer formed on Haynes 230 after exposure for 1500 hours at 650°C. After 500 hours of exposure at 650°C the sample surface is covered mostly with Cr₂O₃ and NiCr₂O₄. This alloy contains about 14wt% of tungsten which give it good corrosion resistance as well as good strength characteristics. The morphology of the oxide protective layer remains almost the same after longer exposure times. The thickness of the protective chromium oxide layer is on the order of only a few hundred nanometers. No significant regions of spallation are observed even at higher exposure times. The data indicate Haynes 230 is a good candidate for high temperature, i.e., ~650°C, applications.

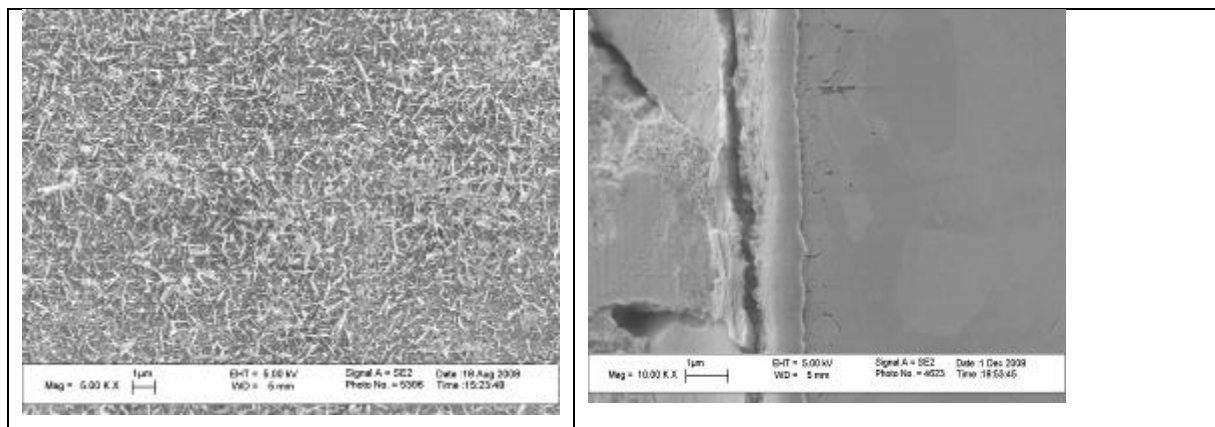


Figure 9. SEM-EDS analysis of the thin, protective oxide layer formed on Haynes 230 after exposure for 1500 hours at 650C, (left) plan view, (right).

316SS & 310SS

Lower grade stainless steels were included in the matrix to look for cost-saving potential and to evaluate their use in the parts of the loop that run at lower temperatures. Alloys and test temperatures are shown in Table 2. Oxide spallation was worse in 316SS than in 347SS and 310SS. The differences in corrosion performance of the alloys has been explained based on the compositions and morphologies of the oxides that form on the surface of the alloys as evaluated by detailed SEM EDS, X-ray diffraction, and XPS analyses. For 316SS, the outer layer consisted of large equi-axed grained Fe₃O₄ (magnetite) and an inner spinel FeCr₂O₄ layer. For the 310SS, Cr rich oxide layers Cr₂O₃ and Cr_{1.4}Fe_{0.7}O₃ improved corrosion resistance. A very thin SiO₂ layer was also observed for 310SS, which is known for its protective qualities. Discontinuous islands of carburized regions were observed underneath the oxide layers which appear to promote delamination of oxide layer from the alloy substrate.

316SS exhibited poor corrosion resistance compared to the different austenitic steels. The oxide layer showed large grains and evidence of spallation. The outer layer of the oxide consisted of magnetite (Fe₃O₄) and the inner layer consisted of (Fe, Cr) spinel oxide layer.

310SS showed significantly better corrosion resistance than 316SS. The structure of the oxide layer was similar in that it consisted of an outer Fe₃O₄ layer and an inner (Fe, Cr) spinel oxide layer. However, as in the case of 316SS, oxide spallation was observed.

Ferritic-martensitic Steels

P91, HCM12A and NF616 were also investigated at 650°C (Figure 10). The plan was for these metals to be examined only at lower temperatures during Phase 2, but these 650°C tests were run because there was space available in the test chamber. As expected, these showed significantly thicker internal oxidation layers than the austenitics and Inconels and are unsuitable for operation at high temperatures. Of the Ferritic-martensitic steels the F91 performed better than the HCM12A.

Summary of Phase 1 Materials Tests

In summary, Table 4 below provides a qualitative upper temperature limit for the tested alloys with some additional comments based on SEM/EDS analysis discussed above. This is a preliminary assessment and more analysis is needed to determine the metric of <30 micron/year attack. Selection of the alloys for the different temperature ranges were loosely based on the anticipated lowest cost material that should be sufficient with respect to corrosion. Any of the alloys that are listed for the higher temperatures are acceptable for lower temperature operation. The recommendations did not include an assessment of the cost and wall thickness for pressure vessel code restrictions. They also did not include creep/rupture since this is dependent on the particular wall thickness and cycling issues. These recommendations are based on current and past corrosion results. The data summarized here form part of two journal articles [16, 17].

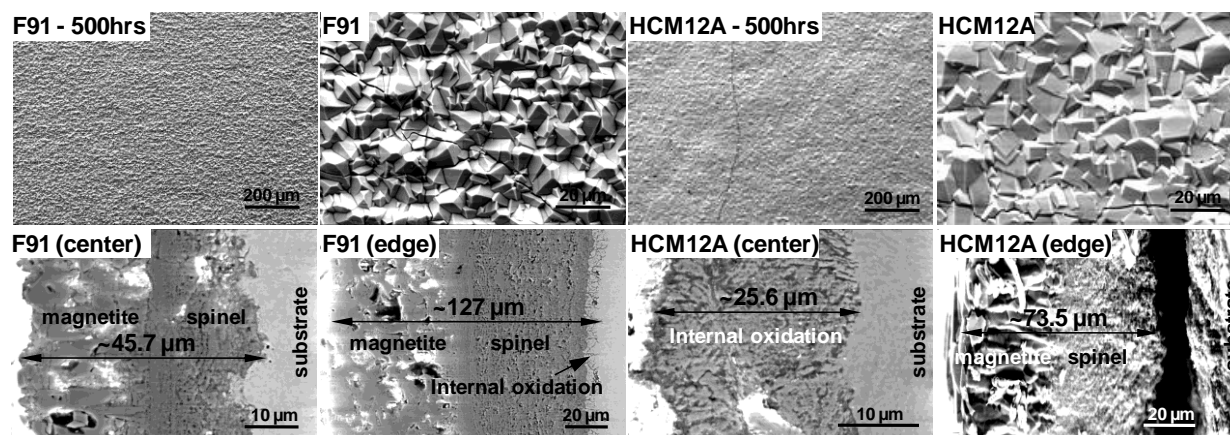


Figure 10. Surface morphologies and cross-sections of F91 and HCM12A samples exposed to S-CO₂ at 650°C for 500 hours.

Table 4. Recommended temperature limit of alloys based on quantitative and qualitative assessment of surface oxidation from s-CO₂ corrosion tests in research grade CO₂ at 20 MPa.

| Temperature [°C] | Pressure [bar] | Recommended Alloy | Comments |
|------------------|----------------|-------------------------------------|--|
| T < 200 | 100 | 304ss, P91 or T22 | For temperatures under 200C ferritic alloys should be usable. |
| T < 250 | 240 | 304ss , P91 | Low cost austenitic or ferritic alloys |
| T < 400 | 240 | 347ss,310ss,304ss or 316ss | Austenitic alloys are recommended. P91 may be suitable for short term periods |
| T < 550 | 240 | 347ss, 310ss | Austenitic are recommended preferably with higher Ni, Cr, Co concentrations (310, 347) 304 or 316 should be suitable for short periods |
| T < 650 | 240 | Haynes 230, IN617, 800H, 347 or 310 | Higher Ni/Cr alloys are recommended 347 or 310 should be sufficient for short time periods |
| T > 650 | 240 | Haynes 282 or IN740 | Little testing completed. Haynes 230 and IN617 may be sufficient for short time periods. |

Task 1.2 Test Plan Development

The purpose of this Task was to outline the commission and test of the SunShot Heat Engine System at the Sandia test site in New Mexico and is based on the EPS100 test program at Dresser-Rand facilities in Olean, NY. The project system was planned as a modification of the Echogen EPS100 system where turbine inlet temperature and compressor inlet temperature would be raised to levels that are relevant to applications in CSP. The basic characterization of the system – control and operation philosophy – would remain the same or be similar for the this program, and the test results of the EPS100 would be utilized to guide the testing of the system.

The test program was aimed at confirming the high temperature power turbine performance and characterizing the system components at these temperatures and during transient operation. The plan called for test data to be recorded continuously. More than thirty temperature, pressure and flow rate measurements were to be recorded at all times. Some component characterization would occur as preliminary tests prior to full operation. A final test plan presented during Phase II would provide the complete details of the experimental conditions.

Table 5. Draft SunShot system test plan

| TPS# | TPS Description | Objectives | Planned Dates |
|------|-----------------|---|---------------|
| 001 | System Checkout | <ul style="list-style-type: none"> • Verify proper installation • Verify there are no leaks • Verify electronics and instruments are working correctly | Q1FY15 |

| | | | |
|-----|---|---|-------------------|
| | | <ul style="list-style-type: none"> • Pressure test of the system | |
| 002 | Controls Check | <ul style="list-style-type: none"> • Verify the controls system is working properly | Q1FY15 |
| 003 | Valve Check | <ul style="list-style-type: none"> • Verify all valves installed and functioning | Q1FY15 |
| 004 | CO ₂ Mass Management System | <ul style="list-style-type: none"> • Verify proper installation • CO₂ storage system commissioning • Verify transfer pump operation • Verify system and valves work correctly | Q1FY15 |
| 005 | Start Pump Circulation | <ul style="list-style-type: none"> • Verify start pump functionality, performance, and controls • Tune start pump control loop • Define control for start pump circulation | Q1FY15 |
| 007 | Air Cooling Characterization | <ul style="list-style-type: none"> • Define transient thermal response of air cooler • Define hydraulic characterization of air cooler | Q1FY15 |
| 008 | Recuperator Characterization | <ul style="list-style-type: none"> • Define transient thermal response of high-temp recuperator • Define of hydraulic characterization of high-temp recuperator • Define transient response of recuperators 2 & 3 | Q1FY15 |
| 009 | Heat Exchanger Check | <ul style="list-style-type: none"> • Define the thermal response of all HXs • Define hydraulic characterization of all HXs | Q1FY15 |
| 010 | Heat Supply and Rejection System Test | <ul style="list-style-type: none"> • Verify the system is working properly • Define thermal response and characterization of the system • System hot start capability | Q1FY15 |
| 011 | Turbo-Compressor Map | <ul style="list-style-type: none"> • Define the functionality of the turbo-compressor • Confirm and measure bearing supply flow • Confirm operation to full speed • Verify design performance • Turbo-compressor map for various conditions (hot and cold days, partial and full power) | Q2FY15- Q3FY15 |
| 012 | Power Turbine Start, Synchronization, and Map | <ul style="list-style-type: none"> • Define the functionality of the power turbine and the synchronization loop • Define control during power turbine start • Confirm operation to full speed • Verify design performance • Power turbine map for various conditions (hot and cold days, partial and full power) | Q2FY15- Q3FY15 |
| 013 | Generator Check | <ul style="list-style-type: none"> • Verify generator functionality and performance | |
| 014 | Performance Test | <ul style="list-style-type: none"> • Verify that the system will remain in continuous operation at full load and typical cycles | Q2FY15- Q3FY15 |

The proposed revised Phase 2 test plan called for testing at a single turbine inlet temperature of 600°C (see *Path Forward* section). Turbine inlet temperature would be controlled by the combustor operation and flow. Investigation of ambient temperature

variation (compressor inlet temperature) would be accomplished by varying the number of operating fans in the air cooling system.

Sandia personnel participating in the test program would be trained on the equipment by Echogen and Echogen personnel would take required training for working at the lab site. The tests at Olean serve as a model for the experimental procedures at Sandia. Staff from other project partners (NREL, Abengoa, and Barber-Nichols) would assist in parts of the operations and receive necessary training. A safety review of the full system would take place before testing commences.

During the test program, changes in the test plan would be at the discretion of the Test Director and testing team. The test team will consist of Echogen test personnel experienced with the operation of the EPS100 and Sandia Laboratory test personnel. At the completion of each test run or day of testing, a review of data would take place. This review would help ensure that proper data were recorded and determine if the team can move on to the next test or must repeat the just completed test.

The final SunShot Program report would include the test data, reduced data and performance analysis, component mapping and comparison of test results to cycle and component analysis.

Task 1.3 Test Loop Design

The basis for the SunShot test loop design was the Echogen EPS100 system, which was under test at the Dresser-Rand facility in Olean, NY. The EPS100 system is a closed-loop s-CO₂ condensing cycle designed for waste heat recovery applications at about 500°C or less. It was planned to modify the turbomachinery of the EPS100 for higher compressor inlet (i.e., dry cooling) and turbine inlet conditions that are representative of CSP applications. The test loop architecture itself would remain unchanged. Use of the existing EPS100 cycle was necessary in order to test the power turbine at reasonable cost. Not only was the s-CO₂ handling system of the EPS100 already developed, but the cycle design allows for extraction of thermal energy from a gas-fired heat source. The power turbine would be tested with a gas-fired heat source because no solar test facility of the necessary size exists and a solar test would be prohibitively expensive. Test cycle efficiency was not a metric of the project; rather, the power turbine performance data would be used to estimate the overall efficiency of an advanced s-CO₂ cycle in a solar application.

The test system was a modification of the Echogen EPS100 system. This avenue represents the best approach to meet the SunShot technology milestones in an expedient, reasonable cost approach. The heat engine itself consisted of three major assemblies: (1) process skid, (2) power skid, and (3) CO₂ storage system. The process skid of the EPS100 is comprised of two recuperators, the turbine-driven pump, control system, valves, and instrumentation. It also holds the cooler if the system is water cooled, although for the SunShot tests an air cooled heat exchanger would be used. The process skid can be operated independently of the power skid by bypassing the majority of the pumped CO₂ back to the cooler inlet.

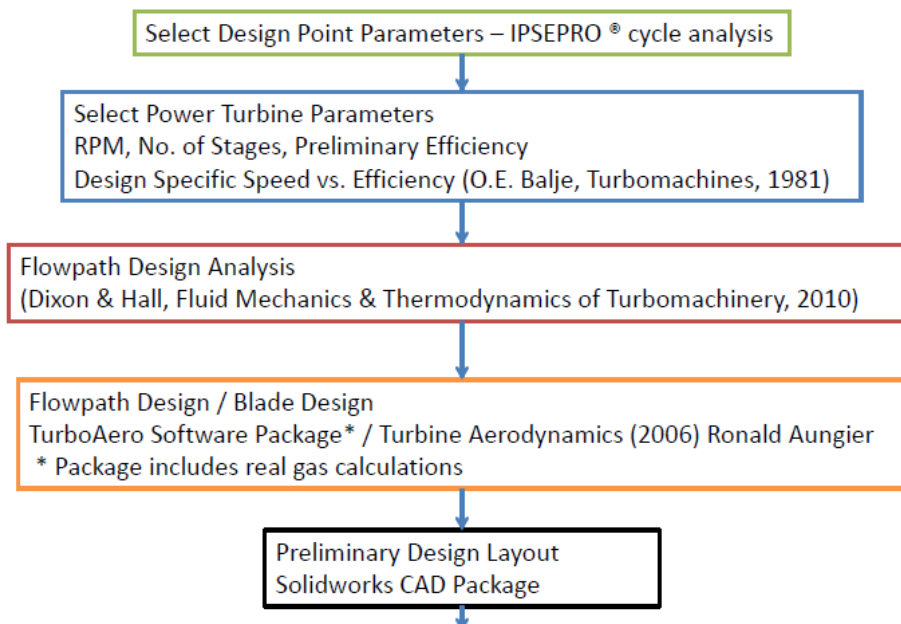
The power skid would contain the power turbine, gearbox, generator, turbine stop valve, and other auxiliary equipment (e.g., seal gas conditioning panel, lubrication system). It receives high-temperature, pressure s-CO₂ from the process skid through the main heat exchanger, and returns the lower temperature and pressure CO₂ after expanding through the power turbine.

The CO₂ storage system would contain sufficient volume of liquid CO₂ to fill and drain the main system, and to provide inventory control for the main fluid loop to permit stable operation of the system under varying heat source, sink and ambient conditions. A transfer pump and controls were also included within the subsystem.

The system is designed to be connected to an external heater and heat sink. Typical applications for the EPS100 include industrial waste heat and gas turbine exhaust heat recovery. Because of the characteristics of typical combustion exhaust, the maximum output power of the heat recovery system is reached by extracting as much heat as possible from the heat source (i.e., reducing the exhaust temperature to as low as practical of a value). The heat source supplies the energy for both the turbocompressor and power turbine.

Power Turbine Design

The power turbine for the EPS100 system is a single-stage radial design. The power turbine for the SunShot program was planned as a scaled prototype of the expected full scale CSP (100 MW size) turbine with similar features. The SunShot power turbine would have a lower efficiency (80%) than expected for a full scale unit (90%) but be designed with similar features, i.e. a multistage axial-flow turbine. The design and manufacture of the SunShot power turbine would utilize current commercial turbomachinery technology. The testing of this unit would then provide a strong foundation and confidence for the progress to full scale systems. The turbine design process is outlined in Figure 11.



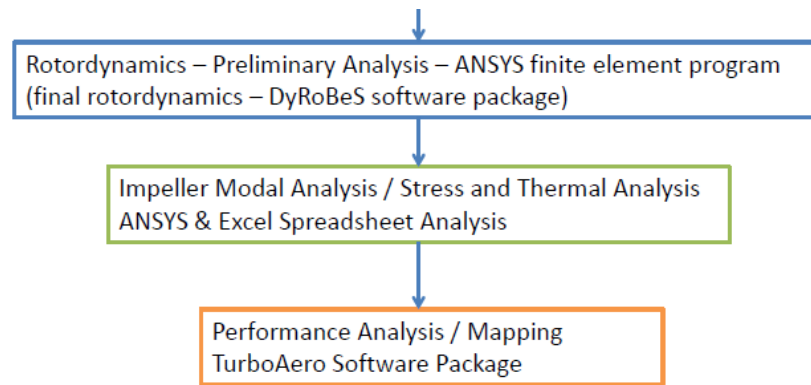


Figure 11. Schematic of the Flowpath for the Turbine Design Process

As is essential for s-CO₂ systems, the IPSEpro cycle software and the turbine design package utilize real gas thermodynamics. TurboAero is a well-accepted, commercial turbine design package. The design process was an iterative process, back and forth through the steps to reach the appropriate design. Design decisions were made based on manufacturability and commercially available components as well as best efficiency and good flowpath practices. The power turbine design requirements Table 6 are defined by the optimization of the SunShot system cycle and maximum operating or material operating conditions.

Table 6. Power turbine design parameters

| Parameter | Value (in) | Value (out) |
|---------------------------------------|------------|-------------|
| Temperature (°C) | 700 | 600* |
| Pressure (MPa) | 23.30 | 10.17 |
| Mass flow rate CO ₂ (kg/s) | 65.2 | 65.2 |

*Based on Balje [13], for a four-stage axial turbine, the efficiency is approximately 0.80.

Materials

Two materials were considered during the design analysis. For the rotating components, the properties of Inconel 718, a nickel-based alloy were utilized. It is an oxidation and corrosion resistant material for service in environments subjected to heat and pressure. Inconel 740 was part of the corrosion test matrix UW-Madison. These two alloys have similar properties at temperatures of 1400°F (760°C). IN718 has a greater yield strength, but IN740 is expected to be more corrosion resistant. Either material is acceptable for turbine components, but because of its expected better corrosion resistance, IN740 was expected to be the preferred choice.

For the turbine housing ASTM A336 Grade 91 was the default. This is a 9% chrome alloy steel composition that Dresser-Rand utilizes in their compressor and turbine casing designs. 347SS has slightly improved strength properties at elevated temperatures and was to be considered during the detailed design process. The preferred design approach was to utilize cooling flowpaths through the turbine housing; this cooling would maintain a temperature where conventional, less-expensive materials can be applied for the SunShot testing.

High Temperature Recuperator

The planned system had a high-temperature recuperator to handle the power-turbine discharge temperature as shown in Table 7. The allowable pressure drop through each side of the recuperator was 0.15 MPa (22 psi).

Table 7. High temperature recuperator requirements

| | Side A | Side B |
|-------------------------|-------------------------|--------|
| Flow Rate (kg/s) | 65.19 | 65.19 |
| Temperature In (°C) | 600 | 387 |
| Temperature Out (°C) | 435 | 553 |
| Inlet Pressure (MPa) | 10.62 | 23.16 |
| Heat (kW) and UA (kW/C) | 10,740 kW and 200 kW/°C | |

The preferred material of construction for the high-temperature recuperator was 316/316L, although it was unclear if this alloy would be suitable and a higher-cost alloy would be required. The manufacturer applies a nominal 0.5 multiplier on the ASME design stress numbers to provide a commercially sensible design pressure limitation. A comparison of different alloy strengths is shown in Figure 12 below. Decreasing the maximum turbine inlet temperature to 600°C or tempering the flow with cooler CO₂ could limit the recuperator inlet temperature to approximately 500°C and allow the entire recuperator to be fabricated from 300-series stainless steel.

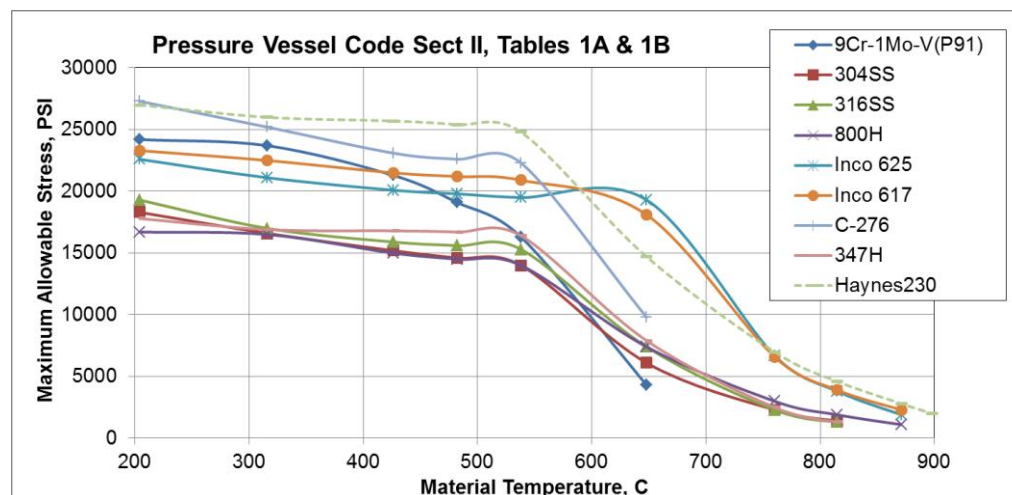


Figure 12. Allowable stress limits for candidate alloys as a function of temperature. Shifting maximum TIT from 700°C to 600°C will allow for use of lower-cost alloys.

Heat Rejection System

An air-cooled heat exchanger (ACHE) system was selected as the best arrangement for the proposed tests. The corresponding air-cooled pre-cooler requirements are shown in Table 8. After reviewing several quotes, Abengoa selected Hammco Air Coolers (Owasso, OK) as the preferred provider. Hammco quoted a 5-bay unit, each bay containing three forced-draft, 13-ft diameter fans. The unit can provide 26.9 MW cooling assuming 100 kg/s CO₂ at 168°C to 42°C and ambient air at 35°C.

A revision of the design point conditions to an ambient air temperature of 33°C and a CO₂ outlet temperature of 45°C was proposed to reduce the ACHE to four bays with a commensurate reduction in capital and operating cost. The reduction in size will preclude testing the system during the hottest summer afternoons in Albuquerque, but this is not expected to impact the test schedule.

Table 8. Air-cooled s-CO₂ precooler design requirements as quoted by Hammco, assuming operation in Albuquerque, NM.

| Parameter | Value (in) | Value (out) |
|--------------------------------|------------|-------------|
| Pressure CO ₂ (MPa) | 10.02 | 10.01 |
| Temp CO ₂ (°C) | 167.8 | 42.2 |
| Mass CO ₂ (kg/s) | 100 | 100 |
| Pressure air (MPa) | 0.0782 | 0.0749 |
| Temp air (°C) | 42.0 | 83.4 |
| Mass flow rate air (kg/s) | 647 | 647 |

Heat Addition System

The test loop system cycle described above was designed around a gas-fired Heat Exchanger (HX) inlet temperature equal to 1000°C with an exhaust gas mass flow rate equal to 35.2 kg/s. The HX was designed with three zones (coils) in series. The resulting HX coil requirements are provided in Table 9.

Table 9. Gas-fired heat exchanger (HX) design requirements

| | HX-Coil #1 | HX-Coil #2 | HX-Coil #3 |
|-----------------------------|------------|------------|------------|
| T hot-in (°C) | 1000 | 714 | 562 |
| T hot-out (°C) | 714 | 562 | 183 |
| P cold-in (MPa) | 23.31 | 23.06 | 23.44 |
| P cold-out (MPa) | 23.30 | 23.05 | 23.39 |
| T cold-in (°C) | 545 | 236 | 75 |
| T cold-out (°C) | 700 | 390 | 200 |
| Mass CO ₂ (kg/s) | 65.2 | 33.2 | 65.2 |
| UA (KW/°C) | 55.8 | 20.0 | 73.0 |

HX material selection is a function of the temperature of the coil in question. T22/T23 steel would be suitable for the low and middle temperature coils. Stainless steel type 347 was proposed in lieu of high-Ni alloys for the high-temperature coil to minimize cost for the short-duration test; however, the corrosion results described under Task 1.1 indicate that 347SS is not a good choice for temperatures at or above 650°C.

The estimated cost for the heater system exceeded the allocation for that device provided in the original project budget. Heater quotes from four different vendors were obtained, ranging from \$3.5 to \$6.4M for the nominal 35 MW_t gas heater. Only one vendor was comfortable quoting a 700°C operating temperature, and that unit was based on an experimental heat exchanger design. The unit was quoted at \$4.4M at

700°C using Inconel 625 and \$3.5M at 600°C using 347SS. The three other vendors quoted a price of \$3.9M and higher for a 600°C unit.

The NREL team proposed reducing the upper temperature to 600°C to reduce materials cost of the fired heater as well as several other system components. Even limiting the upper test temperature to 600°C, the test system exceeded the current funding. Project member EPRI indicated a willingness to contribute an additional \$500,000, but no other team member offered to increase funding.

To deal with this shortfall, NREL initiated discussion with the Southwest Research Institute (SwRI) about combining resources to construct a large, high-temperature s-CO₂ test facility. SwRI was the prime contractor on a similar SunShot-funded project to develop an s-CO₂ turboexpander (DE-EE0005804). SwRI would entertain such an idea only if the facility were located at SwRI. The first step of these discussions was confirmation with all the industry partners from both projects that such a collaboration would be considered. Following this go-ahead, an initial assessment by both teams indicated sufficient synergistic savings to allow construction of a 600°C test facility, and possibly a 700°C test facility. More detail is provided in the *Path Forward* section.

Task 1.4 Modeling and Simulation of Cycles

NREL developed a cycle model of the SunShot test unit in Engineering Equation Solver (EES), and the model showed good agreement with predictions made by Echogen using IPSEpro. As Echogen's development of their IPSEpro model advanced, NREL dropped further development of the EES model and dedicated those resources to addressing the issue of the overall project cost exceeding the planned budget.

In addition to NREL's EES modeling, PhD candidate John Dyreby at UW-Madison modeled the performance of simple and recompression s-CO₂ power cycles at design and off-design conditions. This work resulted in a FORTRAN-based model of the simple and recompression cycle that can be used to optimize design and operating strategy for these cycles [18]. The UW-Madison model indicated that, especially for dry-cooled systems running ~20K above the critical temperature, the efficiency advantage of the recompression cycle only occurs with large recuperator area. This suggests that simpler, lower capital-cost designs might be preferred for the first dry-cooled s-CO₂ power cycles. The tradeoff between complexity and efficiency will also impact the development timeline.

Task 1.5 Commercial Power Cycle

Supercritical CO₂ power cycles have been proposed for a number of applications in which they have perceived advantages. For heat sources that are not dependent upon extraction of sensible enthalpy (e.g. CSP and nuclear), the recompression and partial cooling cycles offer high thermal efficiency, exceeding available steam technology above a turbine inlet temperature in the 450-550°C range, depending on the assumptions used in the analysis. The partial-cooling cycle has been identified as the leading candidate for CSP applications due to its combination of efficiency, recuperator conductance requirements, and temperature differential across the primary heat exchanger [15]. However, commercial implementation of any new technology power cycle will require certain barriers to be overcome. For CSP applications, these are:

- Development and demonstration of key technologies on a component-level
- Development of a pilot-scale system (assumed to be ~ 10 MW for CSP)
- Sufficient pilot-scale operating experience in a relevant environment
- Confidence in scalability of pilot unit to utility sizes

Fortunately, many of the key technologies have been developed, and are being demonstrated by Echogen in their EPS100 waste heat recovery system. These include the heat exchangers, controls, and turbomachinery. The three areas which are not addressed by the EPS100 system are the following:

- **Turbine design.** The current EPS100 power turbine is a single-stage radial design. For the 7.5MW rating of the EPS100, this is the appropriate technology selection. However, at sizes larger than approximately 20MW, multistage axial turbines are the preferable configuration, providing a compact design that can operate at synchronous generator speed.
- **Turbine inlet temperature.** Turbine inlet temperature for exhaust and waste heat recovery applications are typically in the 400-500°C range. Current solar molten salt applications can reach as high as 565°C salt temperature. Advanced CSP systems are expected to operate at temperatures near 700°C to achieve the SunShot efficiency targets.
- **Cycle Design and Efficiency.** The EPS100 cycle architecture was designed to maximize the output power from a heat source that is limited in its total heat availability by the allowable temperature decrease. This results in an architecture that is optimized for energy extraction, not thermal efficiency. A CSP-optimized cycle would be designed for maximum thermal efficiency and integration with thermal energy storage.

The first two issues (as well as demonstration of higher compressor inlet temperatures associated with dry cooling in hot climates) were being directly addressed by the current project. Scaling of the SunShot turbine to a 100 MW class system would follow well-established turbine design principles, guided by the experience gained during the SunShot program.

At the successful conclusion of the current project, the required key technology demonstration milestones for a pilot-scale plant would have been achieved. In order to complete the process towards full-scale commercialization, we anticipate being required to demonstrate a pilot-scale (~5-10 MW) plant in a high-efficiency cycle application.

Commercial development of such a plant is dependent upon securing adequate financial backing, which in turn requires demonstrated pre-commercial deployment. Based on discussions with potential commercial partners, two years of pilot-scale operation was held as a reasonable threshold for obtaining bank financing for a full-scale CSP plant utilizing sCO₂ technology.

Task 1.6 CSP Commercial Deployment Path

The CSP commercial deployment path task included an assessment of different concepts for s-CO₂ integration with CSP. Abengoa defined and analyzed various cases as shown in Table 10 using a combination of IPSEpro and TRNSYS models.

Table 10. Conceptual design matrix for s-CO₂ / CSP system modeling

| <i>Variable</i> | <i>Range</i> |
|---------------------------------------|---|
| s-CO ₂ Power Cycle | <ul style="list-style-type: none"> • Recompression • Partial cooling • Cascaded recompression |
| Receiver Technology (Maximum Temp) | <ul style="list-style-type: none"> • Molten salt HTF trough (550°C) • Molten salt HTF tower (565°C) • Phase change material (PCM) tower (750°C) • Direct s-CO₂ (650°C) |
| Storage | <ul style="list-style-type: none"> • 0, 6, 12, and 15 hours |
| Gross Electric Power Rating | <ul style="list-style-type: none"> • 10 MW, 50 MW, 100 MW |

S-CO₂ Cycle Design-Point Modeling

IPSEpro was utilized to optimize the design point parameters as well as predict the off-design performance of the s-CO₂ power cycles listed in Table 10. Prior to establishing the design point performance, the cycle parameters for each cycle configuration were optimized. After setting bounding constraints on maximum cycle pressure, ambient conditions and minimum main compressor inlet temperature a parametric search over other possible parameter values was performed, and the combination of parameters which yielded the lowest capital cost over production ratio was selected.

Cycle efficiency and ΔT across the solar receiver were noted as key metrics, and Rankine power cycle performance was used as a baseline case. The partial cooling cycle was found to be slightly less efficient than the recompression cycle, but it does benefit from an increased ΔT of $\sim 40^\circ\text{C}$.

After performing the initial simulations, the selection of design ambient and main compressor inlet temperature was found to have a significant impact on the annual S-CO₂ cycle and CSP system performance. Both design temperatures were optimized in subsequent simulations.

Off-Design S-CO₂ Cycle Modeling

The off-design cycle performance was predicted with IPSEpro with the range of operation parameters experienced when coupled to a CSP system. The three operational parameters of interest were: (i) solar HTF inlet temperature to S-CO₂ cycle, (ii) solar HTF mass flow rate to S-CO₂ cycle, and (iii) ambient temperature.

All heat exchangers (excluding the solar HTF heat exchanger) utilized a 1-D discretized model where the log-mean temperature difference was calculated with a given UA product set from the design point simulation. The pressure ratio and efficiency through the compressor(s) were predicted with a relative performance curves given the flow rate

and speed. The mass flow rate and efficiency of the turbine were predicted with a relative performance map given the pressure ratio and speed. Both the relative performance curve and map were created from absolute performance curves/maps supplied by Echogen. Utilizing relative performance allowed the off-design performance at 10, 50, and 100 MWe to be scaled by the design point efficiency alone. The control methodology can be summarized as:

- Inventory control utilized to maintain maximum system pressure of 250 bar by varying the inlet pressure to the main compressor.
- Cooling fans run at full power. At ambient temperatures below the design point, this drops the main compressor inlet temperature below the design point.

CSP S-CO₂ Annual Simulations

The CSP systems described Table 10 were evaluated on an annual transient performance and cost basis by Abengoa using their internal TRNSYS-based cost/performance model. First, each plant was designed to meet the target power ratings at design conditions. DELSOL3 was used for the tower-type solar field and receivers; an internally developed solar field model was used for trough-type solar fields; and internally developed models were used for piping systems, TES equipment, and auxiliary systems. Based on this design, the total plant overnight construction cost was calculated using Abengoa's internal cost models.

Next, the plant's performance was simulated over the course of a year. The solar field optical performance was calculated using DELSOL3 for tower fields and using internally developed performance curves for Abengoa's trough collectors. First-principle-based receiver models were used for both the tower and trough heat collection elements with the exception of the direct s-CO₂ receiver because the design was not completely defined. Piping, TES, and auxiliary system performance and losses were also calculated from first principles. The power cycle performance was evaluated from a lookup table based on the previously described IPSEpro off-design s-CO₂ cycle modeling.

All simulations were conducted with typical meteorological year weather data based on Abengoa's Solana CSP-trough site near Gila Bend, AZ. The transient performance was evaluated on a 15-minute time step basis incorporating thermal inertia, warm up and cool down periods, and maximum system ramp rates. After the annual performance simulations and cost modeling, the System Advisor Model's financial model was used to calculate LCOE with conservative and predicted operations and maintenance cost assumptions.

A control strategy allowing the cooling fans to run at full power even during mild ambient temperatures was found to yield superior performance, because the advantage of the resulting lower compressor inlet temperature (CIT) more than offset the higher parasitic power consumption. The partial-cooling cycle exhibited a lower LCOE despite its lower cycle efficiency due to lower recuperation cost and a larger temperature differential across storage compared to the recompression cycle. The impact of the temperature

differential across storage highlighted the importance of integration with thermal storage conditions.

In summary, the LCOE of conventional molten salt tower technology can be improved by replacing the steam Rankine power block with an s-CO₂ cycle. An 8% LCOE reduction was projected using technologies developed in this project and operating at 600°C. A 13.5% reduction was possible using pure NaNO₃ salt and lower recuperator costs. Pure NaNO₃ has a slightly higher heat capacity and slightly lower cost than the binary NaNO₃ / KNO₃ solar salt. The tradeoff is a higher melting point, but the higher cold tank operating temperature of the s-CO₂ reduces this risk. The recuperator cost reduction potential was estimated on the basis of discussion with teams developing new recuperator designs, including project partner Sandia. Heat exchanger costs have a strong influence on system optimization and cost, and greater understanding is needed regarding the potential for reduction and innovation in these units. A similar optimization of the system assuming a hypothetical HTF capable of operation at 700°C was underway when the project was terminated by DOE.

CSP Roadmap

Commercial deployment of s-CO₂ power cycles for CSP will likely go through two phases due to current CSP deployment economics and the state of heat transfer system development. The objective of the first phase will be to establish s-CO₂ power cycles as a reliable and commercially bankable power cycle technology. Even with anticipated incremental improvements in the efficiency, cost, and off-design performance of these systems we do not expect s-CO₂ cycles to dramatically improve the economics of CSP plants in the 500-565°C range. Operation at salt temperature near 600°C is estimated to provide an 8% improvement in LCOE, with the ability to evolve to higher temperature and efficiency.

Historically, due to limitations in cost or materials, new turbines are first tested at lower temperatures and/or pressures than they ultimately achieve. Standard flow similarity conditions (similitude) are used to model turbine behavior and predict performance at other operating conditions.

For example, if we run a performance test of the power turbine at some inlet pressure and inlet temperature other than the design inlet temperature and pressure, we can plot the data in terms of pressure ratio (P_{in} / P_{out}) vs. equivalent mass flow, $\dot{m}_{eq} = \dot{m} * T^{1/2} / P_{in}$, for lines of equivalent speed, $N_{eq} = N / T^{1/2}$. Also, we can plot efficiency vs. equivalent mass flow or pressure ratio for lines of equivalent speed. Data taken at similar equivalent speeds will fall on the same line (see Figure 13). These correlations allow us to project the performance at any other inlet pressure or temperature.

This type of approach is used to provide component performance without testing at each and every data point and is proposed here to allow for testing of the prototype turbine while staying within project budget.

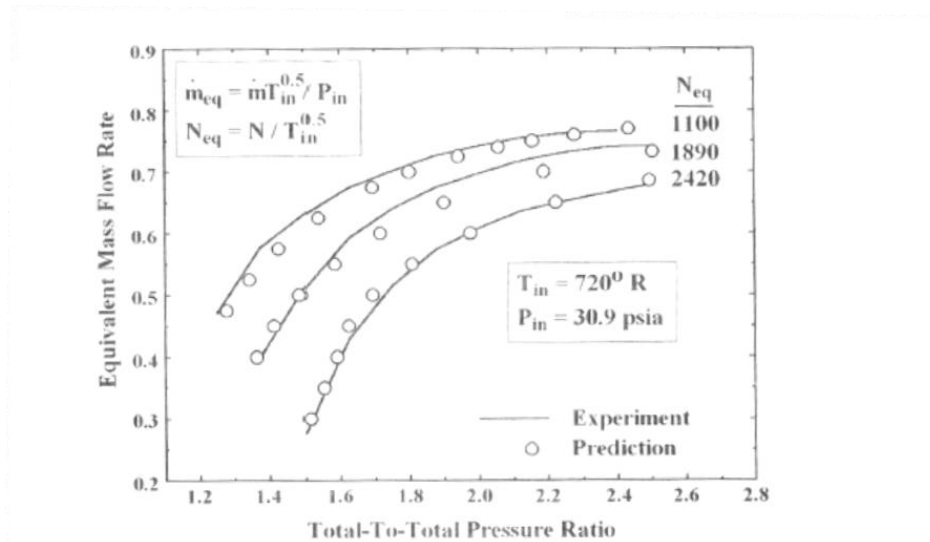


Figure 13. Plot of equivalent mass flow vs. pressure ratio showing lines of constant equivalent speed [15].

In the second step, higher temperature cycles that significantly differentiate the performance of s-CO₂ cycles from steam Rankine cycles will be deployed with newer CSP technologies, potentially including novel molten salts, particle receivers, molten or phase change metals, and other HTFs. The objective of this phase of deployment is to use s-CO₂ cycles to enable high-efficiency, low-cost CSP plants for long-term commercial deployment. This timeline depends on these HTF technologies progressing through the same small-scale testing that the s-CO₂ cycles will undergo through this project. Once the s-CO₂ cycle and the higher temperature HTF technologies have been demonstrated individually, they can be deployed together with synergistic effect.

Utility Stakeholder Workshop

An EPRI-hosted workshop on s-CO₂ technology occurred on July 31, 2013. This workshop helped familiarize utilities with the potential of the s-CO₂ power cycle and explored possible early adopter sites. The workshop queried representatives from 18 different utilities regarding the perceived benefits and threats to the s-CO₂ cycle. Perceived benefits included: thermal efficiency, partnership opportunities with customers, distributed generation opportunities (potentially non-utility), potential for lower cost capital equipment, modularity, load following capability, benign working fluid, ability to be coupled with a variety of heat sources; and small-scale commercial applications are feasible and can generate useful operating data leading up to full-scale power generation applications.

Results of the survey indicated the greatest concerns of the potential utility users are: technical readiness, system capital cost, material durability, and scale-up uncertainty. Each of these concerns was being addressed to some degree in the project.

Task 1.7 Site Preparation

The planned host site for the test was the Nuclear Energy Systems Lab (NESL) at Sandia National Laboratory in Albuquerque, NM. During Phase 1 Sandia made preparations to run a natural gas extension to NESL to fuel the approx. 35 MW_t fired-

heater for the test system. Sandia assessed three different options for power offtake from the planned test: use of a mechanical water or air brake, renting electrical load banks, or connection to the local grid. Mechanical brakes were quickly discarded due to the size of the unit and Echogen's prior poor experience with water brake reliability. The grid-tie option was attractive for long-term operations at the site and was of interest to Sandia, but the time and cost to install a power substation was prohibitive for this project's needs. Ultimately, electrical load banks were selected as the best option. Quotes were obtained from different vendors and ComRent (Owings, MD) was selected. Rental of a 10 MWe load bank set, including connecting cabling and shipping, for six months was \$552,000 and those costs were incorporated into the Phase 3 cost estimates for a test period of 25 weeks.

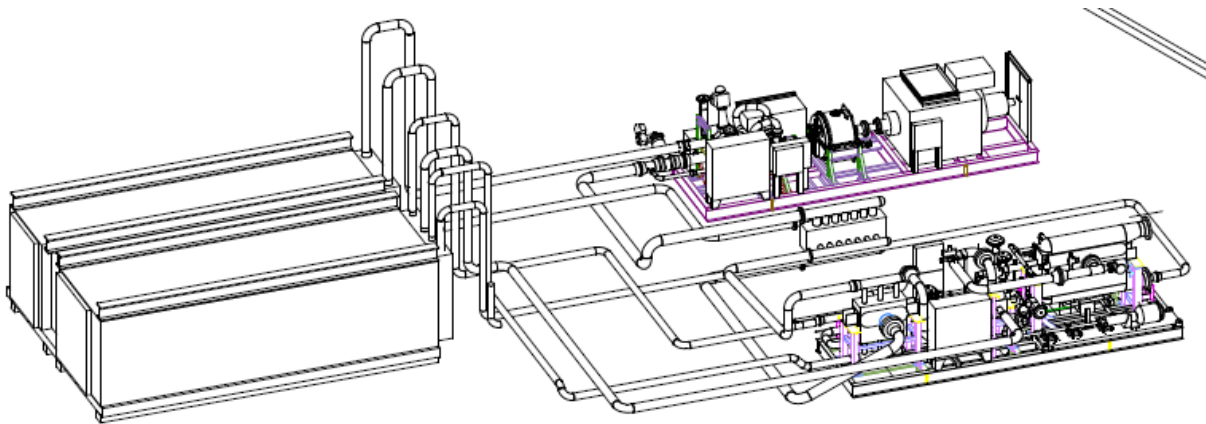


Figure 14. Isometric view of the process skid, recuperator, power skid, and fired heater heat exchanger showing interconnection piping. Skids measure approx. 11 ft x 36 ft.

An air permit would be required for the gas burner, but was not anticipated for the precooler. Experience indicated that a permit will require 6-12 months from application to issue. Once the completed design of the furnace is available, Sandia planned to resume talk with Albuquerque Air Quality to complete the process.

The budget overrun for the fired-heater made testing at Sandia unlikely without an infusion of additional funds. Combining with the project led by SwRI in San Antonio was a viable option, but requires relocation to San Antonio, TX. More information on that prospect is provided in the *Path Forward* section.

Conclusions

The 10 MW s-CO₂ Turbine project was a major development effort with multiple partners and significant hardware requirements. The project brought together a diverse and complementary set of stakeholders with the common goal of advancing the s-CO₂ power cycle technology toward commercial deployment. The three-phase project called for system design in Phase 1, followed by fabrication in Phase 2, and testing in Phase 3. The major accomplishments of Phase 1 included:

- Design of the s-CO₂ power turbine and turbocompressor, which built upon the engineering and test results of the Echogen EPS100 system,
- Update of equipment and installation costs,
- Development of simulation tools for the test loop itself and more efficient cycle designs that are of greater commercial interest,
- Simulation of s-CO₂ power cycle integration into existing (<600°C) molten salt CSP systems indicating a cost benefit of up to 8% in LCOE,
- Recuperator cost was identified as a key economic parameter.
- Corrosion data for multiple alloys at temperatures up to 650°C in high-pressure CO₂ and recommendations for materials-of-construction for the test unit, and
- Draft plan and preliminary operating conditions based on the ongoing tests of the EPS100 in Olean, NY.

The project included four cost-sharing partners: DOE/EERE, Echogen, Abengoa, and EPRI, as well as indirect support from the DOE/NE program. Maintaining a balance between the specific interests of these partners and the overall goal of advancing this power generation technology was critical to the success of the program. While the accomplishments described above were considerable, Phase 1 incurred many challenges. Most significant of these was the cost of the supporting hardware to drive this large-scale test. Table 11 lists the Phase 1 accomplishments relative to the specific SOPO milestones. The following *Path Forward* section outlines the proposed path to continue the project in a fashion planned to accomplish our primary objectives within the available resources. However, DOE opted to terminate the work.

Table 11. Phase 1 milestone summary

| Milestone | Phase 1 Results | Status |
|--|---|---------------|
| 1.1 Alloy test matrix; recommendation for test loop materials | Completed testing of candidate alloys at 1000 hrs and conditions up to 200 bar and 650°C in research grade CO ₂ . Recommendations listed in Table 4. | ✓ Achieved |
| 1.2 Test Plan and draft SOP. | Operating procedures and test plan mirror that in-use for the EPS100 and used for Sandia's smaller-scale tests. Test schedule revised and re-budgeted. Test outline provided in Table 5. | ✓ Achieved |
| 1.3.1 Test loop 100% design completed; 80% turbine and 80% compressor | Test loop design completed, but estimated cost exceeds planned budget, primarily due to the fired heater. The lowest heater cost assumes a derate of the test temperature from 700°C to 600°C and use of a new heat exchanger design. Power turbine and turbocompressor unit designs complete and projected to meet efficiency targets. | ✓ Achieved |

| | | |
|---|--|--------------------|
| efficiencies | | |
| 1.3.2 Turbomachinery design study for 100 MW scale | A multistage, axial-flow power turbine selected as a scale model of the 100 MW design. Nondimensional similarity to the 10 MW unit indicate a synchronous design with >90% isentropic efficiency. | ✓ Achieved |
| 1.4.1 Transient performance model of test loop | Steady-state design and off-design models developed for the test cycle, as well as the simple and recompression cycles. IPSEpro adopted by Echogen and Abengoa for cycle modeling. NREL transient model development terminated as Echogen assumes greater role in cycle modeling. | ✗ not achieved |
| 1.5 Review commercial power cycle design | Partial-cooling cycle viewed as best CSP-relevant cycle design due to combination of efficiency, total recuperator cost, and temperature differential across thermal storage. Technical scale-up path understood, but commercial development path uncertain due to softening of U.S. CSP market. | Partially achieved |
| 1.6 Deployment roadmap to SunShot | Near-term application of s-CO ₂ power cycle with ~100 MW molten salt tower viewed as probable development path. First deployment at 585°C to 600°C allows match with solar salt to minimize risk; but shows only small benefit vs. steam Rankine on annual basis. Near-term benefit will be needed to justify industry investment. Progression to 700°C evolves with system experience. | Partially achieved |
| 1.7 Draft NEPA assessment | Existing Sandia NEPA accommodates 10-MW scale test. Equipment layout and installation costs estimated. Permit for fired heater defined and will be applied for at outset of Phase 2. | ✓ Achieved |

Path Forward:

The greatest threat to the project was the greater-than-expected cost of the support infrastructure, primarily the cost for the gas-fired heater that supplies thermal energy to the test system and costs associated with installation of the equipment. In addition, the cost for electric load banks exceeded expectations.

In the July 31, 2013, Phase 1 continuation report, NREL proposed a path forward incorporating the following changes from the originally proposed project:

1. Reduction of the turbine inlet temperature from a max value of 700°C to 600°C.
2. Change from two test campaigns at 550°C and >650°C to a single campaign at 600°C.
3. Elimination of NREL/Sandia cycle modeling Tasks 2.4 and 3.4.
4. Elimination of test support for Sandia’s small recompression loop (Task 3.5).

The decrease in turbine inlet temperature to 600°C has a dramatic effect on material properties and associated component costs. At the same time, the proposed test conditions still achieved the important advance of an axial-flow turbine design while remaining highly relevant to solar applications. For example, a 600°C solar-salt power tower is consistent with Kolb’s 2011 analysis of next-generation molten salt power towers [14].

Viability of the proposed path forward was contingent on acquiring a 600°C fired heater at a cost of approximately \$2M, or securing additional funds for the hardware

procurement. However, in the period between July 31 and the September 30 Phase 1 end date, neither of these contingencies was realized.

In the interim, NREL identified an alternative path that involved collaborating with a related SunShot-funded project to build a shared test facility. Discussion between the two project teams revealed that neither NREL nor the team led by SwRI could afford the infrastructure required for testing a multi-MW s-CO₂ power turbine – an objective both projects shared. Combining infrastructure resources would provide the ability to develop a test facility of sufficient size to test high-temperature, s-CO₂ power systems at multi-MW scale. Such a facility would be a significant asset to the government and industry as they work to develop and commercialize this new technology. After securing the support of all the industry partners, the general approach and benefits of a collaborative effort were presented to DOE in November:

- Combining resources enables construction of large s-CO₂ test facility. A 7-MW, 600°C facility is clearly achievable within current cost estimates and test plans. Neither project can afford such a facility if pursued individually.
- A more advanced, 700°C facility is possible, but requires additional analysis:
 - Further refinement of fired heater and high-temperature recuperator costs,
 - Assessing use of an air-brake to simplify energy dissipation and turbine change-out,
 - Examining flow bypass to reduce turbine stop valve cost, and
 - Refining test plan requirements.
- The project would test two power turbine designs at near full-flow and temperature conditions
- Such a test facility would be a significant asset for DOE's planned Supercritical Transformational Electric Power (STEP) pre-commercial demo plant. Testing at the joint facility would reduce STEP project risk.

The projected budget situation of the individual and combined projects is presented in Table 12. After reviewing the collaborative presentation, DOE decided not to entertain a joint project proposal and terminated the s-CO₂ Turbine Test Project on December 6, 2013. Although DOE opted not to allow the teams to pursue a joint test facility, the researchers and industry members from both teams concur that such a facility is needed for further development of the s-CO₂ power cycle. Validation of turbine performance at the multi-MW scale is believed to be the required next step for the technology. Testing and cost reduction in high-temperature, high-pressure recuperators is another demonstration need that would have been served by the proposed work.

The culmination of the research program would require operational demonstration of a high-efficiency s-CO₂ Brayton cycle to validate the commercial readiness of the new power technology. This goal is outside the work scope proposed here, but is consistent with the DOE STEP program.

Table 12. Budget for proposed Phase 2 and 3 activities.

| Budget for Phases 2 and 3 | | Estimate Cost (600C with 347SS) | | Estimated Cost (700C with IN625) |
|---------------------------|--|---------------------------------|----------------|----------------------------------|
| Task | Description | Original Budget | | |
| 2.1 | Corrosion and Materials | \$ 150,716 | \$ 150,716 | \$ 150,716 |
| 2.2 | Test loop construction | 8,184,819 | 11,064,000 | 11,964,819 |
| 2.3 | Site Preparation, Installation, and Checkout** | 225,000 | 1,192,600 | 1,192,600 |
| 2.4 | Modeling and Simulation | 71,676 | 71,676 | 71,676 |
| 2.5 | Conceptual Design and Cost Study | 314,483 | 314,483 | 314,483 |
| 3.1 | Corrosion and Materials | 60,495 | 60,495 | 60,495 |
| 3.2 | Low-temp operation | 2,174,000 | 2,597,540 | 2,597,540 |
| 3.3 | High-temp operation (>650C) | 2,124,000 | - | 835,100 |
| 3.4 | Performance Model Validation | 235,663 | - | - |
| 3.5 | Response and Control of Recompression cycle | 209,309 | - | - |
| | ** 347SS assumed for interconnection piping | \$ 13,750,161 | \$ 15,451,510 | \$ 17,187,429 |
| | Differential | | \$ (1,701,349) | \$ (3,437,268) |
| | With additional EPRI contribution | 500,000 | \$ (1,201,000) | \$ (2,937,000) |
| | With estimated SwRI project contribution | 2,166,000 | \$ 965,000 | \$ (771,000) |

References:

[1] Angelino, G., "Carbon Dioxide Condensation Cycles for Power Production", ASME Paper No. 68-GT-23, (1968).

[2] Dostal, V., "A Supercritical Carbon Dioxide Cycle for Next Generation Nuclear Reactors," Ph.D. Thesis, Dept. of Mechanical Engineering, Massachusetts Institute of Technology, 2004.

[3] Dostal, V., and M. Kulhanek, "Research on the Supercritical Carbon Dioxide Cycles in the Czech Republic," Supercritical CO₂ Power Cycles Symposium, Troy, NY, April 29-30, 2009.

[4] Kulhánek, M., and V. Dostal, "Thermodynamic Analysis and Comparison of Supercritical Carbon Dioxide Cycles," Supercritical CO₂ Power Cycle Symposium, Boulder, CO, May 24-25, 2011.

[5] Parma, E.J., S.A. Wright, M.E. Vernon, D.D. Fleming, G.E. Rochau, A.J. Suo-Anttila, A. Al Rashdan, and P.V. Tsvetkov, "Supercritical CO₂ Direct Cycle Gas Fast Reactor (SC-GFR) Concept, Sandia National Laboratories, SAND2011-2525, May 2011.

[6] Turchi, C.S., Z. Ma, T. Neises, and M. Wagner, "Thermodynamic Study of Advanced Supercritical Carbon Dioxide Power Cycles for High Performance Concentrating Solar Power Systems," Proceedings of ASME 2012 6th International Conference on Energy Sustainability & 9th Fuel Cell Science, Engineering and Technology Conference, July 23-26, 2012, San Diego, CA, USA.

[7] Wright, S.A., T.M. Conboy, E.J. Parma, T.G. Lewis, G.A. Rochau, and A.J. Suo-Anttila, "Summary of the Sandia Supercritical CO₂ Development Program," SCO₂ Power Cycle Symposium, Boulder, Colorado, May 24-25, 2011a.

[8] Sienicki, J.J., A. Moisseytsev, R.L. Fuller, S.A. Wright, and P.S. Pickard, "Scale Dependencies of Supercritical Carbon Dioxide Brayton Cycle Technologies and the Optimal Size for a Next-Step Supercritical CO₂ Cycle Demonstration," Supercritical CO₂ Power Cycles Symposium, Boulder, CO, May 24-25, 2011.

[9] Was, G.S., and S. Teyseyre, "Challenges and Recent Progress in Corrosion and Stress Corrosion Cracking of Alloys for Supercritical Water Reactor Core Component," Proc. 12th Int'l Conf. Environmental Degradation of Materials in Nuclear Power Systems – Water Reactors, American Nuclear Society, Salt Lake City, UT., pp. 1343- 1357, 2005.

-
- [10] Holmes, D.R., and Hill, R.B., "Corrosion of Steels in CO₂," British Nuclear Energy Society (BNES), Reading University, 1974.
- [11] Kofstad, P., and Bredesen, R., "On the Oxidation of Iron in CO₂+CO Gas Mixtures II: Reaction Mechanisms during Initial Oxidation," *Oxidation of Metals*, Vol. 35, Nos. 1-2, pp. 107-137, 1990.
- [12] Zhang, J., Speck, P., and Young, D.J., "Metal Dusting of Alumina-Forming Creep Resistant Austenitic Stainless Steels," *Oxidation of Metals*, Vol. 77, pp. 167-187, 2012.
- [13] Balje, O.E., *Turbomachines*, John Wiley & Sons, 1981.
- [14] Gregory J. Kolb, "An Evaluation of Possible Next-Generation High-Temperature Molten-Salt Power Towers," SAND2011-9320, Sandia National Laboratories, December 2011.
- [15] Neises, T., and C. Turchi, "A comparison of supercritical carbon dioxide power cycle configurations with an emphasis on CSP applications," SolarPACES 2013, Las Vegas, NV, September 17-20, 2013.
- [16] Leng, B., Roman, P., Sridharan, K., Anderson, M., "Corrosion behavior of 316 and 347 stainless steels in supercritical CO₂ of different purity," *Corrosion Science*, submitted September 2013.
- [17] Lingfeng, He, Roman, P., Sridharan, K., Anderson, M., "Multi-scale characterization of corrosion behavior of alumina forming austenitic steels exposed to supercritical carbon dioxide," *Corrosion Science*, submitted September 2013.
- [18] Dyreby, J. J., Klein, S. A., Nellis, G. F., and Reindl, D. T., "Modeling Off-Design and Part-Load Performance of Supercritical Carbon Dioxide Power Cycles," *Proceedings of ASME Turbo Expo 2013*, No. GT2013-95824, pp. 1-7, 2013.